HHS Public Access

Author manuscript

Nat Microbiol. Author manuscript; available in PMC 2018 November 28.

Published in final edited form as:

Nat Microbiol. 2018 February ; 3(2): 243–252. doi:10.1038/s41564-017-0065-7.

Activation of *Vibrio cholerae* quorum sensing promotes survival of an arthropod host

Layla Kamareddine[#1], **Adam CN Wong**[#1,2], **Audrey S. Vanhove**[1], **Saiyu Hang**[1,3], **Alexandra E. Purdy**[1,4], **Katharine Kierek Pearson**[1], **John M. Asara**[5,6], **Afsar Ali**[7,8], **J. Glenn Morris Jr.**[7], and **Paula I. Watnick**[1,9]

[1]Division of Infectious Diseases, Boston Children's Hospital, Harvard Medical School, 300 Longwood Avenue, Boston, MA 02115, U.S.A.

[2]Current address: Department of Entomology and Nematology, University of Florida, 1881 Natural Area Drive, Gainesville, FL 32608, U.S.A.

[3]Current address: University of Massachusetts Medical School, 364 Plantation Street, Worcester, MA 01605, U.S.A.

[4]Current address: Department of Biology, AC #2237, Amherst College, PO Box 5000, Amherst, MA 01002, U.S.A.

[5]Division of Signal Transduction/Mass Spectrometry Core, Beth Israel Deaconess Medical Center, 3 Blackfan Circle, Boston, MA 02115, U.S.A.

[6]Department of Medicine, Harvard Medical School, Boston, MA 02115, U.S.A.

[7]Emerging Pathogens Institute, University of Florida, P.O. Box 100009, 2055 Mowry Road, Gainesville, FL 32610, U.S.A.

[8]Department of Environmental & Global Health, School of Public Health and Health Profession, University of Florida Gainesville, FL 32610 U.S.A.

[9]Department of Microbiology and Immunobiology, Harvard Medical School, 77 Avenue Louis Pasteur, Boston, MA 02115, U.S.A.

[#] These authors contributed equally to this work.

Abstract

Vibrio cholerae colonizes the human terminal ileum to cause cholera and the arthropod intestine and exoskeleton to persist in the aquatic environment. Attachment to these surfaces is regulated by

Corresponding author: Paula I. Watnick, Telephone: (617) 919-2918 Fax: (617) 730-0254 paula.watnick@childrens.harvard.edu.

Author Contributions: L. K., A. C. N. W, A. S. V., S. H, J. M. A., and P. I. W. designed the experiments. L. K., A. C. N. W., A. S. V., S. H., and J. M. A. performed the experiments. K. K.-P., A. E. P., A. A., and J. G. M. Jr. contributed critical reagents. L. K., A. C. N. W., A. S. V., S. H., J. M. A., and P. I. W analyzed the data. P. I. W. wrote the manuscript. All authors reviewed, edited, and approved the manuscript.

Data Availability:

Metabolomic data generated during this study is available in the supplementary information files of this manuscript. Other data that support the findings of this study are available from the corresponding author upon request.

Competing financial interests: The authors declare no competing financial interests.

the bacterial quorum sensing signal transduction cascade, which allows bacteria to assess the density of microbial neighbors. Intestinal colonization with *V. cholerae* results in expenditure of host lipid stores in the model arthropod *Drosophila melanogaster*. Here we report that activation of quorum sensing in the *Drosophila* intestine retards this process by repressing *V. cholerae* succinate uptake. Increased host access to intestinal succinate mitigates infection-induced lipid wasting to extend survival of *V. cholerae*-infected flies. Therefore, quorum sensing promotes a more favorable interaction between *V. cholerae* and an arthropod host by reducing the nutritional burden of intestinal colonization.

Keywords

Vibrio cholerae; quorum sensing; succinate; Drosophila melanogaster; metabolism; host-microbe interaction; biofilm

Introduction

In a process known as quorum sensing, bacteria produce small molecules termed autoinducers that accumulate in the environment as a function of cell density. Upon reaching a particular concentration threshold, these autoinducers alter collective bacterial gene transcription in a fashion that is hypothesized to be adaptive. Quorum sensing may thus allow a bacterium to respond to environmental conditions as a multicellular rather than unicellular organism. Behaviors that benefit from coordinated multicellular action include utilization of available nutrients [1, 2], surface attachment or biofilm formation [3–5], natural competence [6–8], and regulation of virulence and symbiosis strategies [9, 10]. Quorum sensing by the human diarrheal pathogen *Vibrio cholerae* modulates all of these [1, 5, 11, 12].

V. cholerae is adapted to the human intestine and the aquatic environment, two very different milieus. Colonization of the human small intestine, a region of the gut with a relatively low burden of commensal bacteria [13], is dependent on the toxin co-regulated pilus (TCP) [14]. Cholera toxin (CTX), which is synthesized in the small intestine, then induces the osmotic diarrhea of cholera [15, 16]. *V. cholerae* also lives in close proximity to arthropods in terrestrial, estuarine, and fresh water environments [17–21]. The *V. cholerae* biofilm exopolysaccharide VPS enables this pathogen to accumulate on abiotic surfaces and colonize the arthropod exoskeleton and intestine [22–24]. TCP, CTX, and VPS are all repressed at high cell density by the quorum sensing circuitry [5, 11, 12, 25]. The quorum sensing signaling cascade also promotes proteolytic degradation of environmental phages, resistance against grazing by amoebae and flagellates, and persistence within the amoebal contractile vacuole [26–28]. Here we show that *V. cholerae* quorum sensing is activated in the *Drosophila* intestine and attenuates pathogen virulence as a result of decreased succinate uptake. This quorum sensing-regulated reduction in bacterial succinate transport delays host expenditure of triglycerides, reproductive organ atrophy, and death. Taken together, our studies suggest that a functional *V. cholerae* quorum sensing system benefits both host and pathogen by minimizing the nutritional impact of infection.

Results

The *V. cholerae* quorum sensing master regulator HapR represses biofilm matrix synthesis in the *Drosophila* intestine at high pathogen burden.

The *V. cholerae* quorum sensing master regulator HapR decreases *V. cholerae* biofilm formation at high cell density due to transcriptional repression of the *vps* genes, which encode the VPS synthesis machinery [5, 11, 22]. To confirm this phenotype in the quorum sensing-competent strain C6706 originally isolated from Peru in 1991, we measured biofilm formation in a C6706 Δ*hapR* mutant [29] (Fig. 1a). *V. cholerae* VPS-dependent biofilm formation is required for colonization of the *Drosophila* gut by the quorum sensing-deficient clinical strain MO10 [24, 30]. We questioned whether wild-type C6706, which forms very little biofilm in a test tube, could colonize the *Drosophila* intestine. To measure this, we performed a colonization transfer experiment in which the fly is given access to *V. cholerae* resuspended in PBS for 48 hours, transferred to sterile PBS for 24 hours to allow for expulsion of unattached *V. cholerae*, surface sterilized, and homogenized. After the wash-out period, *Drosophila* exposed to wild-type C6706 as well as the Δ*hapR* mutant remained colonized, while those exposed to the Δ*hapR* Δ*vpsA* mutant did not (Fig. 1b). We then gave flies access to wild-type and mutant *V. cholerae* expressing the green fluorescent protein (GFP) from a chromosomal location, removed the intestines, and assessed colonization by fluorescence microscopy. As shown in Figure 1c, wild-type C6706 and the Δ*hapR* mutant were abundant in both the midgut and rectum of the fly, while the C6706Δ*hapR*Δ*vpsA* mutant colonized these regions only minimally. This demonstrates that the quorum-sensing competent *V. cholerae* strain C6706 forms a VPS-dependent biofilm in the *Drosophila* intestine. To determine whether high cell density, HapR-dependent repression of biofilm formation was ultimately activated in this setting, we measured *vpsL* gene expression in the intestines of flies colonized with wild-type C6706 or a Δ*hapR* mutant. In fact, transcription of *vpsL* was much higher in flies infected with a C6706Δ*hapR* mutant, demonstrating that HapR represses *vps* gene transcription, not only on abiotic surfaces but also in the colonized fly intestine (Fig. 1d). These data are consistent with a model in which quorum sensing-competent *V. cholerae* initially accumulate in the *Drosophila* intestine. When high cell density is reached, HapR represses transcription of genes that promote colonization.

Quorum sensing attenuates *V. cholerae* virulence.

We questioned whether quorum sensing might also limit pathogenesis. In fact, deletion of *hapR* accelerated host death without significantly increasing intestinal colonization (Fig. 1e-f). We previously showed that diminution of intestinal stem cell division accompanies infection with MO10 [31]. To determine the effect of C6706 and a Δ*hapR* mutant on host intestinal stem cell proliferation, we quantified cells with phosphorylated histone 3 (PH3), a cell division marker (Fig. 1g). Stem cell division was preserved in the intestines of flies infected with wild-type C6706 but not the Δ*hapR* mutant. These results suggest that *V. cholerae* quorum sensing prevents infection-induced arrest of epithelial renewal.

A functional quorum sensing cascade is retained in Haitian strains.

An intact quorum sensing pathway is variably found in *V. cholerae* species isolated from the clinic and the environment [30]. Whether these spontaneous quorum sensing mutations

accumulate in the field or laboratory is unknown. We hypothesized that quorum sensing should be preserved over time if it provided a selection advantage in natural environments. In October of 2010, a quorum sensing-competent strain from Southeast Asia was introduced into the Haitian population and environment as the result of an index case of cholera contracted in Nepal and disseminated in the Artibonite valley [32–34]. This provided the unique opportunity to track inactivation of *V. cholerae* quorum sensing after introduction and dispersal in a new environment [35]. To study this, we deleted *hapR* in Haitian strains isolated between 2010 and 2013 and assessed biofilm formation. As shown in Figure 2a, biofilm formation was greatly increased in Δ*hapR* mutants. As additional strains became available over the course of our studies, they were tested, and these also exhibited repression of biofilm formation by HapR (Supplementary Fig.1). Similar to strain C6706, we observed minimal mortality in *Drosophila* infected with Haitian strains but equivalent or higher bacterial burdens as compared with the quorum sensing-deficient clinical strain MO10 (Fig. 2b-c). Furthermore, we did not detect a significant difference in the total burden of commensal bacteria in the intestines of infected and uninfected flies (Fig. 2d). We conclude that decreased virulence is not the result of a *V. cholerae* colonization defect or a change in the number of commensal microbiota. As observed for C6706, deletion of *hapR* in the Haitian strains accelerated the mortality of infected flies and suppressed intestinal stem cell division (Fig. 2e-f). Taken together, our findings suggest that quorum sensing-regulated repression of *V. cholerae* virulence in this host is retained over years and possibly decades.

Biofilm formation is not responsible for the increased virulence of *V. cholerae* Δ*hapR* mutants.

We previously showed that *V. cholerae* biofilm formation contributes to virulence in the fly model [24]. To determine whether the increased virulence of the Δ*hapR* strains was due to activation of biofilm formation, we created Δ*hapR*Δ*vpsA* double mutants, which are unable to form a biofilm. The virulence of the Δ*hapR*Δ*vpsA* double mutants was similar to that of the Δ*hapR* mutants (Fig. 2g-i). This suggests that an aspect of HapR regulation other than repression of biofilm formation is responsible for the increased virulence of the Δ*hapR* mutants.

Quorum sensing impacts pathogen nutrient uptake and metabolite secretion.

Mutation of both *V. cholerae* acetyl-CoA synthase (Acs1) and the glycine cleavage system (Gcv) reduces virulence in the MO10 quorum sensing-defective background due to decreased bacterial uptake of the survival-prolonging metabolites acetate and methionine sulfoxide, respectively [36–38]. However, when *Drosophila* are simultaneously infected with equal numbers of MO10Δ*acs1* and Δ*gcvT* mutants, rapid mortality comparable to that of the parental strain ensues because each mutant consumes the life-extending metabolite that the other cannot [36]. We hypothesized that quorum sensing might similarly prolong host survival by sparing a life-extending metabolite not spared by a quorum sensing-defective strain. To test this, we first co-infected flies with MO10 and each of the Haitian strains. Consistent with our hypothesis, co-infected flies expired at rates similar to that of MO10-infected flies (Supplementary Fig. 2a). To determine whether the metabolite spared by quorum sensing strains was related to acetate or methionine sulfoxide, we performed co-infections with MO10Δ*acs1* or Δ*gcvT* mutants. We found that co-infection with any of the Haitian strains

and the MO10Δ*gcvT* mutant led to rapid death, comparable to that of the wild-type MO10 infection (Fig. 3a-d). This was not the result of one strain outcompeting its partner (Supplementary Fig. 2b-d). This suggests that the Haitian strains may consume or reduce extracellular methionine sulfoxide, the metabolite spared by the MO10Δ*gcvT* mutant, in the fly intestine. In contrast, co-infection of Haitian strains with the MO10Δ*acs1* mutant resulted in a survival phenotype similar to solo infection with either of the infecting strains. These data suggest that co-infection with any Haitian strain and the MO10Δ*acs1* mutant results in accumulation of a survival-prolonging metabolite. To determine whether this metabolite was acetate, we quantified acetate uptake by the Haitian *V. cholerae* strains and corresponding Δ*hapR* mutants cultured in LB broth. Both parental and mutant strains consumed acetate quite rapidly as compared with the MO10Δ*acs1* mutant (Fig. 3e-h). This suggested that acetate was not the survival-prolonging metabolite associated with Haitian strains, that increased consumption of acetate does not underlie the augmented virulence of Δ*hapR* mutants, and, finally, that the Δ*acs1* mutant is unable to consume the survival-prolonging metabolite associated with Haitian strains.

To identify other differentially consumed metabolites, we performed metabolomic analysis on the spent supernatants of the Haitian strain isolated in 2013 and the corresponding Δ*hapR* and Δ*hapR* Δ*vpsA* mutants (Supplementary Table 1 and 2). Although biofilm formation did not significantly alter the virulence of the Δ*hapR* mutants, we hypothesized that it might alter their metabolism. We first identified several small molecules present in significant quantities that were differentially consumed by the Δ*hapR* mutant as compared with the wild-type strain and the Δ*hapR* Δ*vpsA* mutant (Fig. 3i). These findings demonstrate that biofilm formation is associated with consumption of a unique set of metabolites that do not alter virulence. These metabolites were eliminated from further study. We then identified small molecules that were consumed by the Δ*hapR* and Δ*hapR* Δ*vpsA* mutant strains but not the parental strain (Fig. 3j). We hypothesized that uptake of one or more of these metabolites could be responsible for the increased virulence of the Δ*hapR* and Δ*hapR* Δ*vpsA* mutants.

Quorum sensing represses *V. cholerae* succinate uptake to prolong host survival.

Glutamate, succinate, and threonine, metabolites that were nearly completely consumed by the Δ*hapR* mutants, were investigated. To identify metabolites whose uptake by the Δ*hapR* mutant were responsible for increased virulence, we prepared LB medium supplemented with glutamate, succinate, and threonine in 5 mM concentrations and infected flies with the Δ*hapR* mutant in this medium. As shown in Figure 3k, supplementation significantly prolonged survival of flies infected with a Δ*hapR* mutant. We then exposed flies to LB inoculated with the Δ*hapR* mutant and supplemented with additional mixtures of metabolites and found that, in each case, increased survival was correlated with the presence of succinate in the mixture (Supplementary Fig. 2e). To test the efficacy of succinate in prolonging survival, we performed infections with the Δ*hapR* mutant in the presence of succinate alone, which did not impact *V. cholerae* growth (Supplementary Fig. 2f). Increased survival was observed, which was greater when succinate was added later in infection (Fig. 3l).

Because succinate uptake was increased in the Δ*hapR* mutant, we hypothesized that the *V. cholerae* succinate uptake transporter Vc INDY might be repressed by HapR [39]. Indeed, we

found that transcription of the gene encoding Vc INDY was increased 3-fold in the Δ*hapR* mutant (Supplementary Fig. 2g). We propose a model in which HapR represses *V. cholerae* succinate uptake at high cell density, resulting in an increase in dietary succinate available to the host.

Our data suggest that the MO10Δ*acs1* mutant does not consume succinate. Interestingly, acetyl-CoA, the product of Acs1, and succinate are key substrates of the tricarboxylic acid (TCA) cycle. One possibility is that intracellular levels of these two carboxylic acids are linked.

Quorum sensing and succinate preserve adipose tissue lipid stores during *V. cholerae* infection.

Infection-induced depletion of lipids from the *Drosophila* adipose tissue known as the fat body along with accumulation of large lipid droplets in the intestine is correlated with host mortality [36, 38]. To determine whether lipid re-distribution also occurred during infection with the Haitian *V. cholerae* strain, we assessed triglyceride accumulation in the *Drosophila* fat body after four days of access to LB alone or inoculated with *V. cholerae*. As compared with flies fed sterile LB, lipid stores in the fat bodies of flies infected with wild-type *V. cholerae* decreased less than those in the fat bodies of flies colonized with a Δ*hapR* mutant (Fig. 3m). Furthermore, supplementation with succinate increased the lipid stores of flies infected with the Δ*hapR* mutant (Fig. 3m). To determine if this was accompanied by the accumulation of large lipid droplets in the gut, we examined the intestines of flies infected with *V. cholerae* 2013 and the Δ*hapR* mutant strain alone or supplemented with succinate on the fourth day of infection. No accumulation of lipid droplets was observed in the intestines of these flies (Supplementary Fig. 3). This suggests that accumulation of lipid droplets in the gut does not drive depletion of fat body stores during *Drosophila* infection with the Δ*hapR* mutant.

We hypothesized that quorum sensing might promote conservation of host triglyceride stores. To test this, we performed quantitative assays of total triglycerides (Fig. 3n). This confirmed our hypothesis. Furthermore, while there was a trend towards rescue of triglyceride stores with succinate supplementation, this did not reach statistical significance after adjustment for multiple comparisons. Total glucose and protein were not significantly different among the conditions tested (Fig. 3o-p), and succinate supplementation in the absence of infection had no effect on lipid accumulation (Supplementary Fig. 4a-b) and did not alter total glucose or triglyceride stores (Supplementary Fig. 4c-d). This demonstrates that *V. cholerae* quorum sensing and succinate ingestion affect lipid stores in host adipose tissue specifically in the setting of infection.

Succinate ingestion does not impact host appetite.

We tested the possibility that quorum sensing and succinate might augment lipid stores by increasing *Drosophila* food intake during infection. The flies differentially avoided consumption of the Δ*hapR* mutant. However, by day 4, this difference in consumption was minimal (Supplementary Fig. 5a-b). Furthermore, succinate supplementation had no effect

on food intake. These data do not support the hypothesis that quorum sensing and succinate modulate lipid stores through an effect on appetite.

A transcriptional response indicative of starvation is not observed during infection with a quorum sensing mutant.

Succinate is a key intermediate in the TCA cycle [40, 41]. We hypothesized that enterocyte succinate depletion due to pathogen ingestion of this metabolite might inhibit the TCA cycle, thus activating a starvation response. In an MO10 infection, we found that intestinal transcription of *ImpL2*, *lnR*, and *dilp6* was activated and insulin signaling was extinguished, a pattern indicative of enterocyte starvation [38, 42–44]. This was reversed by mutation of *acs1* or *gcvT* (Supplementary Fig. 5c-d) [38]. We questioned whether quorum sensing might also redirect bacterial metabolism to prevent enterocyte and host starvation. In fact, transcription of these genes either in the gut (Supplementary Fig. 5e-g) or in whole flies (Supplementary Fig. 5i-k) was not significantly altered on the fourth day after exposure to the Haitian *V. cholerae* strain, the corresponding Δ*hapR* mutant, or the Δ*hapR* mutant supplemented with succinate, and insulin signaling, as evidenced by phosphorylation of the serine/threonine kinase AKT, was not decreased (Supplementary Fig. 5m). Succinate supplementation similarly did not alter *dilp6* transcription in the setting of starvation (Supplementary Fig. 5h-I). Taken together, these data suggest that quorum sensing and succinate supplementation do not impact enterocyte or host starvation in the setting of intestinal *V. cholerae* colonization.

Quorum sensing and succinate supplementation minimally impact host anabolic functions.

Succinate is also a substrate for the anabolic functions of gluconeogenesis and lipogenesis [40, 41]. We hypothesized that quorum sensing and succinate supplementation might promote one of these processes. As the first committed step in gluconeogenesis and glyceroneogenesis, phosphoenolpyruvate carboxykinase (PEPCK) decarboxylates and phosphorylates oxaloacetic acid in the cytoplasm. In addition, acetyl-CoA carboxylase (ACC) catalyzes the first committed step in fatty acid synthesis, the carboxylation of acetyl-CoA to form malonyl-CoA. PEPCK and ACC activity is regulated at the transcriptional level [45, 46]. Transcription of PEPCK was decreased by approximately a factor of 2 in the whole bodies but not intestines of flies infected with the Δ*hapR* mutant as compared with *V. cholerae* 2013 regardless of succinate supplementation (Supplementary Fig. 5n-p). This likely contributes to the decrease in lipid accumulation in the fat bodies of flies infected with the Δ*hapR* mutant but does not reflect a response to succinate. Transcription of *Acc* was unchanged in the bodies and intestines of flies infected with wild-type *V. cholerae,* a Δ*hapR* mutant alone, or Δ*hapR* mutant in the presence of succinate (Supplementary Fig. 5o-q). This suggests that quorum sensing and succinate do not rescue fly survival through transcriptional activation of gluconeogenesis or lipogenesis.

V. cholerae quorum sensing and succinate do not activate the *Drosophila* HIF1-α homolog Sima.

Succinate is a signaling molecule through its interaction with specific transcription factors and G-protein coupled receptors. It has been demonstrated to stabilize the α subunit of the hypoxia-inducible factor (HIF1-α) [47]. In *Drosophila*, the HIF1-α homolog Sima represses

signaling through the IMD pathway. We predicted that activation of the IMD pathway in the setting of infection with a quorum sensing-competent *V. cholerae* strain might be decreased as compared with a quorum sensing-defective strain due to succinate stabilization of Sima. Because the IMD pathway activates transcription of antimicrobial peptides including Diptericin [48], we measured *diptericin* transcription to assess output through the IMD pathway. However, HapR and succinate supplementation had no effect on *diptericin* transcription (Supplementary Fig. 5r-s).

Evidence that intestinal succinate extends host survival by inhibiting lipolysis.

We then hypothesized that infection with the *V. cholerae* 2013Δ*hapR* mutant might specifically activate lipolysis, and, furthermore, that quorum sensing and succinate might prolong host survival of infection by preventing this. To test this, we blocked lipolysis by two independent mechanisms. *Drosophila* insulin-like peptide 6 (Dilp6) and Brummer (Bmm), an essential lipase, are required for triglyceride mobilization from the fat body [42, 49]. To determine whether reduction of *dilp6* and *bmm* expression in the fat body might increase host resistance to infection, we obtained a bmm^1 heterozygote, two independent *dilp6* RNAi constructs, and a *bmm* RNAi construct. We used these tools to decrease *dilp6* and *bmm* transcription in the fat body (Supplementary Fig. 6a-c) and then measured resistance to infection. As shown in Figure 4a-b and Supplementary Figure 6d, knockdown of *dilp6* in the fat body increased host survival of infection but did not alter intestinal colonization. In addition, total triglyceride stores of flies infected with a 2013 Δ*hapR* mutant were similarly increased by knockdown of *dilp6* and succinate supplementation (Fig. 4c). In this genetic background, we also observed a small but significant decrease in total glucose concentration as a result of infection, which was more pronounced in the Δ*hapR* mutant infection, but *dilp6* knockdown in the fat body and succinate supplementation did not rescue glucose levels (Fig. 4d). Bodipy staining revealed triglyceride retention in the fat body without accumulation in the intestine (Fig. 4e-f). Flies with *bmm* knocked down in the fat body as well as bmm^1 heterozygotes displayed a phenotype very similar to that of $dilp6^{RNAi}$ flies. They were resistant to infection with the 2013Δ*hapR* strain (Supplementary Fig. 6d-g), and lipids were observed in the fat body but not the gut during infection (Supplementary Fig. 7). These results support our contention that quorum sensing prolongs the *V. cholerae*-arthropod interaction by reducing infection-activated catabolism of host lipid stores.

Quorum sensing and succinate supplementation preserve host reproductive organ size and triglyceride accumulation.

We noted that infection with a Δ*hapR* mutant caused the *Drosophila* ovaries to shrink (Supplementary Fig. 8a). This was reminiscent of *Drosophila* ovaries that shrink as a result of increased programmed cell death and decreased cell proliferation [50]. Consistent with this, while the structure of ovarioles from flies infected with the parental *V. cholerae* strain were normal in appearance, the ovariole nuclei of those infected with the Δ*hapR* mutant strain were shrunken and disorganized (Supplementary Fig. 8b). Succinate supplementation increased ovary size and restored normal morphology (Supplementary Fig. 8). We hypothesized that disruption of normal oogenesis might be due to modulation of lipid accumulation in the developing oocytes. Indeed, using Bodipy staining, we noted that the developing oocytes of Δ*hapR*-infected flies were dramatically depleted of lipid stores. This

was also reversed by succinate supplementation. We conclude that *V. cholerae* high cell density HapR-dependent signaling represses pathogen succinate uptake in the intestine, thus increasing host access to this dicarboxylic acid. This, in turn, prevents expenditure of host lipid stores, maintains reproductive organ size, and protects the host against infection-induced mortality.

Discussion

Quorum sensing is a means of interbacterial communication effected by secretion of small molecules that coordinate bacterial behavior under conditions of high cell density [51]. It has been shown to afford biofilm-associated *V. cholerae* resistance to consumption by amoebae and flagellates and may aid the persistence of *V. cholerae* within the amoeba contractile vacuole [26, 27]. Here we show that the *V. cholerae* master regulator HapR is activated in the intestine of infected *Drosophila* and reduces pathogen virulence by repressing transcription of the bacterial succinate transporter. Decreased *V. cholerae* succinate uptake increases host access to this metabolite, which prevents mobilization of host lipid stores and death.

V. cholerae quorum sensing pathways rapidly accumulate spontaneous inactivating mutations [52, 53]. Here we show that after the introduction of a single pathogenic *V. cholerae* strain into Haiti in 2010, quorum sensing competence was retained in a random selection of isolates over a period of six years in spite of evidence for diversification of other parts of the genome under positive selection [35]. This suggests that quorum sensing may provide a selection advantage to the bacterium.

While *V. cholerae* quorum sensing is not a proven component of a host-microbe symbiosis, the concept of quorum sensing as a symbiosis factor in the interaction of *Vibrio* species with environmental hosts is well-established [54, 55]. *V. fischeri* colonization of the squid *Euprymna scolopes* light organ is essential for light organ development [56–58]. Quorum sensing-regulated *V. fischeri* luminescence within this organ then protects the squid from predators [59]. Aquatic and terrestrial arthropods are thought to play an important role in survival of *V. cholerae* in the environment [17–19, 60, 61]. We show here that, at high cell density, *V. cholerae* quorum sensing represses the intestinal colonization factor VPS and mitigates the metabolic demands placed by this pathogen on its arthropod host.

Quorum sensing-mediated repression of *V. cholerae* succinate uptake has the potential to impact metabolism through multiple avenues in both mammals and arthropods. Similar to other TCA cycle intermediates, succinate participates in post-translational modification of lysine residues in proteins [62]. Second, succinate stabilizes the hypoxia-induced transcription factor HIF1-α, which promotes weight gain and obesity in mice [63] and suppresses the innate immune response [48, 64]. Last, the mammalian G-protein coupled receptor GPR91 or SUCNR1, which inhibits lipolysis in response to extracellular succinate, is abundant in cells of the intestinal brush border [65–67]. SUCNR1 mutant mice have less white adipose tissue and are resistant to succinate-induced inhibition of lipolysis, a host phenotype similar to the one reported here to be activated by *V. cholerae* quorum sensing [68]. We conclude that *V. cholerae* quorum sensing is not only a means of interbacterial communication but also an avenue through which a non-invasive intestinal bacterium may exert control over host

metabolic pathways to extend the host-pathogen interaction and prolong environmental dispersal.

Methods

Bacterial strain and fly stocks.

Bacterial strains and fly stocks used are listed in Supplementary Table 3. *V. cholerae* strain MO10 and the corresponding mutants with in-frame deletions in the genes encoding acetyl-CoA synthase (*acs1*) and glycine cleavage system protein T (*gcvT*), were used for co-infection and gene transcription experiments [38]. With the exception of UAS-*dilp6*-RNAi stocks (constructs 3987 and 111727), which were obtained from the Vienna *Drosophila* Resource Center, fly lines were obtained from the Bloomington *Drosophila* stock center.

Drosophila husbandry and bacterial culture.

Fly stocks were maintained on standard fly food containing 16.5 g/L yeast, 9.5 g/L soy flour, 71 g/L cornmeal, 5.5 g/L agar, 5.5 g/L malt, 7.5% corn syrup and 0.4% propionic acid in a 12:12 light:dark cycle incubator at 25°C. *Vibrio cholerae* strains were cultured in Luria-Bertani (LB) broth or on LB agar supplemented with streptomycin (100 μg/ml) at 27°C. Where noted, supplements were added in a 5mM concentration (Sigma).

Generation of *V. cholerae* deletion mutants.

Suicide plasmids carrying in-frame deletions in *hapR* (VC0583) and *vpsA* (VC0917) were constructed using gene splicing by overlap extension and ligation into pWM91 [69, 70]. The primers used to construct the *vpsA* and *hapR* deletions are listed in Supplementary Table 4. In-frame deletions of *hapR* and *vpsA* were engineered into *V. cholerae* by homologous recombination using the suicide plasmids designed for this purpose as previously described [71].

Drosophila infections.

Because of their larger size, female flies were used to maximize material for assays. An overnight culture of *V. cholerae* was diluted in a 1:10 ratio into fresh LB broth. In an arthropod containment level 2 facility, thirty 5 to 7-day-old adult, female flies with genetic background as stated and listed in Supplementary Table 3 were randomly distributed into three fly vials containing a cellulose acetate plug infiltrated with 3 ml of this bacterial suspension. For succinate treatment, 5 mM succinate-containing LB was fed to adult female flies with or without *V. cholerae* infection as noted for each experimental condition. Flies were scored for survival twice daily, harvested for bacterial counts, or dissected for microscopic analysis.

In vitro, in vivo, and microscopic assessments of bacterial growth and colonization.

To assess *in vitro* growth, overnight *V. cholerae* cultures were diluted to an OD_{655} of 0.01 and distributed into microtiter wells in triplicate. The OD_{655} was recorded over time using an Infinite 200 spectrophotometer (Tecan). To assess host bacterial burden, replicates of ten flies were washed three times in ethanol followed by three washes in phosphate buffered

saline (PBS) and homogenized in 500 μl of LB broth at 48h post-infection. The resulting homogenates were diluted, plated on LB agar, and incubated at 37 °C for enumeration of *V. cholerae* or plated on de Man, Rogosa, and Sharp (MRS) agar and incubated at 30 °C for enumeration of gut commensals. Colony forming units/fly were assessed after 24 and 48 hours. In graphs of bacterial burden, each point represents one cohort of ten flies. Colonization transfer experiments, including both enumeration and visualization of bacterial burden, were performed as previously described [24].

Biofilm Assays.

Biofilm formation was quantified as previously described [72, 73]. Briefly, *V. cholerae* cultures were adjusted to an OD_{655} of 0.005 in LB broth and aliquoted into borosilicate tubes in triplicate. The tubes were incubated for 48 hours at 27°C. Planktonic cells were removed and quantified by OD_{655}. The remaining surface attached cells were resuspended in PBS by vortexing with 1-mm-diameter glass beads (BioSpec Products, Inc.) for approximately 1 min [30% (vol/vol)]. The density of the resulting suspension was quantified by OD_{655}.

Immunofluorescence to detect cells containing phosphorylated histone 3 (PH3).

Numbers of $PH3^+$ cells were quantified following 72 hours of exposure to *V. cholerae.* Intestines were removed and fixed with 4% formaldehyde in phosphate-buffered saline + 0.1% Tween 20 (PBST) overnight at 4°C. After washing in PBST three times, tissues were blocked in 2% BSA in PBST for 1 hour at RT and incubated overnight at 4°C with a 1:500 dilution of a rabbit anti-PH3 antibody (Millipore, CA 92590). After two PBST washes, a 1:200 dilution of a goat anti-rabbit antibody conjugated with Alexa Fluor® 594 (Invitrogen) and 4,6-diamidino-2-phenylindole (DAPI, 1 μg/ml) were added to the tissues and incubated for 2 hours at room temperature. After the final PBST wash, tissues were placed in mounting medium (Vector Laboratories) and examined by fluorescence microscopy using a Leica TCS SP2 AOBS system to quantify $PH3^+$ cells per gut.

Metabolomic analyses.

Acetate levels in *V. cholerae* culture supernatants were measured as previously described using an acetate kinase-based kit (Megazyme) following the protocol provided by the manufacturer [38]. To prepare supernatants for polar metabolite analysis, bacterial strains were cultured in triplicate overnight in LB broth at 25°C. Cultures were centrifuged, and the supernatant was removed and filtered through 0.22 μm filter disk (Fisher), dessicated in 80% methanol at ambient temperature in a SpeedVac concentrator (Savant), and subjected to metabolomics analysis as previously described [74]. MetaboAnalyst 2.0 free online software was used for normalization and statistical analysis of data [75]. Metabolomics data were normalized to sum, and a baseline of 0.01 was established. Data were log-transformed prior to calculation of statistical significance using a one-way ANOVA with a false discovery rate of 0.05. A Fisher's Least Significant Difference post-hoc analysis was performed. Normalized data are provided in Supplementary Table 1. Significantly different metabolites are listed in Supplementary Table 2. Metabolomics experiments were performed once.

Lipid Staining.

The fat bodies, intestines, and ovaries of adult flies were dissected at four days post-infection. Tissues were fixed with 4% formaldehyde in PBST, rinsed three times in PBST, and incubated with BODIPY 493/503 (1mg/mL, Invitrogen) and DAPI (1:1000, Invitrogen) for 1 h at room temperature. Confocal images were taken using a Zeiss LSM 780 confocal microscope. These experiments were performed twice with similar results.

Nutritional assays.

Flies were exposed to *V. cholerae* for four days in three separate vials considered biological replicates, harvested, and homogenized in 100 μl Tris-EDTA buffer supplemented with 0.1% Triton X-100. 10 μl of the supernatant was collected immediately and stored at −80°C for total protein quantification, while the remaining suspension was incubated at 90°C for 20 min to inactivate fly enzymes before proceeding with glucose and triglyceride quantification. Total protein, triglycerides, and glucose were quantified using commercial kits and reagents according to the manufacturers' protocols [DC Protein Assay kit, Bio-Rad, Triglyceride Assay kit (Sigma), and Glucose (GO) Assay kit (Sigma)]. These experiments were performed twice with similar results.

Intestinal contents:

The volume of food in the *Drosophila* intestine was quantified as previously described using a fluorescein-based assay [38].

Quantification of gene-specific mRNA levels in bacteria.

For C6706 measurements, triplicate bacterial cultures were grown from separate single colonies. Overnight cultures were harvested and lysed with lysozyme. RNA was extracted using TRIzol (Invitrogen). 500 ng RNA was used for the cDNA synthesis (Invitrogen SuperScript III), and an equivalent amount of RNA was used for genomic DNA control. For measurements of transcription in the Haitian strain 2013, triplicate bacterial cultures were adjusted to an OD_{655} of 0.01 in 2ml LB broth and cultured for 24 hours at 27°C. RNA was extracted using a High Pure RNA isolation kit (Roche Life Science). cDNA synthesis was performed using a Superscript III reverse transcription kit according to the manufacturer's instructions (Invitrogen). For all experiments, q-PCR was performed using iTaq SYBR Green (Bio-Rad) on a StepOnePlus real-time PCR system (Applied Biosystems). The *clpX* gene was used as an internal control. Primers are listed in Supplementary Table 4.

Quantification of gene-specific mRNA levels in *Drosophila*.

For *Drosophila*, thirty to forty-five female flies divided equally into three vials were used for mRNA quantification. These were considered three biological replicates. For validation of RNAi knockdown, whole flies were used. For intestine-specific transcription, intestines were dissected and removed 42 hours after exposure to *V. cholerae*. RNA was extracted using a High Pure RNA isolation kit (Roche Life Science) and treated with TURBO DNase treatment (Ambion). Quantification of total RNA was done with a NanoDrop 1000 spectrophotometer (Thermo Fisher Scientific), and quality was monitored by agarose gel electrophoresis. 500 ng of the resulting RNA was used for cDNA synthesis using a

Quantitech Reverse transcription kit (Qiagen). Real time q-PCR was performed on the StepOnePlus real-time PCR system (Applied Biosystems) using iTaq Universal SYBR Green supermix (Bio-Rad). Relative expression was calculated using the 2-ΔΔCq method. RP49 (CG7939) gene transcription level was used for normalization. Primers used are listed in Supplementary Table 4.

Western Blot analysis.

Ten whole female flies (5–7 days old) were homogenized in PBS (Teknova P0191). Protein samples were reduced and denatured in SDS-PAGE sample buffer (BioRad 161–0747) for 20 min 95°C, separated on a 4–20% polyacrylamide gel (BioRad 456–1096) and transferred to a PVDF membrane (BioRad 1704272). Extracts were immunoblotted with rabbit anti-AKT (1:1000, Cell Signaling Technologies 9272), rabbit anti-Ser505-phospho-dAKT (1:1000, Cell Signaling Technologies 4054), mouse anti-β-Tubulin (1:2500, Developmental Studies Hybridoma Bank AB_579794), anti-mouse and anti-rabbit IgG horseradish peroxidase-conjugated secondary antibodies (1:5000, Cell Signaling Technologies, 7074 and 7072, respectively).

Statistical analysis:

In determining sample size, we relied on extensive experience, while taking into account availability of reagents, feasibility, and expense. Investigators were not blinded to group allocation. In all experiments, the investigators were aware of the experimental condition under investigation. Except where noted, experiments were repeated at least twice with similar results. Measurements represent the mean of at least three biological replicates in all graphs, and error bars represent the standard deviation. As noted and appropriate, a two-tailed students t test, a Welch's t test (unequal variance), a Mann-Whitney test (non-parametric), or a one way ANOVA with Dunnett's test as a post-hoc analysis were used to calculate significance. P values are shown above the relevant measurements. Log-rank analysis was used to assess differences in survival curves. For all tests, a $p<0.05$ was considered significant. Where an indication of significance is not noted, differences between measurements were not statistically significant. Statistical analysis of metabolomics data is detailed in the metabolomics section.

Supplementary Material

Refer to Web version on PubMed Central for supplementary material.

Acknowledgements:

Microscopy was performed at the Microscopy Resources on the North Quad (MicRoN) core facility at Harvard Medical School. This work was supported by National Institutes of Health Grants R21 AI109436 (P.I.W.) and R01 AI097405 (J. G. M.). Many stocks obtained from the Bloomington Drosophila stock center (NIH P40OD018537) and Vienna Drosophila resource center were used in this study. This work was partially supported by NIH grants 5P30CA006516 (J.M.A.) and 5P01CA120964 (J.M.A.). The authors thank Dr. Susanne Breitkopf and Min Yuan for help with mass spectrometry experiments. We thank Dr. Ronald Taylor for sharing strain C6706 with us. This skilled and generous scientist has left a great mark on the field and a void in our hearts.

References

1. Hawver LA, Giulietti JM, Baleja JD & Ng WL Quorum Sensing Coordinates Cooperative Expression of Pyruvate Metabolism Genes To Maintain a Sustainable Environment for Population Stability. MBio 7 (2016).
2. Studer SV, Mandel MJ & Ruby EG AinS quorum sensing regulates the *Vibrio fischeri* acetate switch. J Bacteriol 190, 5915–5923 (2008). [PubMed: 18487321]
3. Hassett DJ et al. Quorum sensing in *Pseudomonas aeruginosa* controls expression of catalase and superoxide dismutase genes and mediates biofilm susceptibility to hydrogen peroxide. Mol Microbiol 34, 1082–1093 (1999). [PubMed: 10594832]
4. Vuong C, Gerke C, Somerville GA, Fischer ER & Otto M Quorum-sensing control of biofilm factors in *Staphylococcus epidermidis*. J Infect Dis 188, 706–718 (2003). [PubMed: 12934187]
5. Hammer BK & Bassler BL Quorum sensing controls biofilm formation in *Vibrio cholerae*. Mol Microbiol 50, 101–104 (2003). [PubMed: 14507367]
6. Ansaldi M & Dubnau D Diversifying selection at the *Bacillus* quorum-sensing locus and determinants of modification specificity during synthesis of the ComX pheromone. J Bacteriol 186, 15–21 (2004). [PubMed: 14679219]
7. Cheng Q, Campbell EA, Naughton AM, Johnson S & Masure HR The com locus controls genetic transformation in *Streptococcus pneumoniae*. Mol Microbiol 23, 683–692 (1997). [PubMed: 9157240]
8. Suckow G, Seitz P & Blokesch M Quorum sensing contributes to natural transformation of *Vibrio cholerae* in a species-specific manner. J Bacteriol 193, 4914–4924 (2011). [PubMed: 21784943]
9. Miyashiro T & Ruby EG Shedding light on bioluminescence regulation in *Vibrio fischeri*. Mol Microbiol 84, 795–806 (2012). [PubMed: 22500943]
10. Rutherford ST & Bassler BL Bacterial quorum sensing: its role in virulence and possibilities for its control. Cold Spring Harb Perspect Med 2 (2012).
11. Zhu J & Mekalanos JJ Quorum sensing-dependent biofilms enhance colonization in *Vibrio cholerae*. Dev Cell 5, 647–656 (2003). [PubMed: 14536065]
12. Lo Scrudato M & Blokesch M The regulatory network of natural competence and transformation of Vibrio cholerae. PLoS Genet 8, e1002778 (2012). [PubMed: 22737089]
13. Neale G, Gompertz D, Schonsby H, Tabaqchali S & Booth CC The metabolic and nutritional consequences of bacterial overgrowth in the small intestine. Am J Clin Nutr 25, 1409–1417 (1972). [PubMed: 4571741]
14. Taylor RK, Miller VL, Furlong DB & Mekalanos JJ Use of phoA gene fusions to identify a pilus colonization factor coordinately regulated with cholera toxin. Proc Natl Acad Sci U S A 84, 2833–2837 (1987). [PubMed: 2883655]
15. Mekalanos JJ, Collier RJ & Romig WR Simple method for purifying choleragenoid, the natural toxoid of *Vibrio cholerae*. Infect Immun 16, 789–795 (1977). [PubMed: 892899]
16. Finkelstein RA & LoSpalluto JJ Pathogenesis of experimental cholera. Preparation and isolation of choleragen and choleragenoid. J Exp Med 130, 185–202 (1969). [PubMed: 4978880]
17. de Magny GC et al. Role of Zooplankton Diversity in *Vibrio cholerae* Population Dynamics and in the Incidence of Cholera in the Bangladesh Sundarbans. Applied and environmental microbiology 77, 6125–6132 (2011). [PubMed: 21764957]
18. Broza M, Gancz H, Halpern M & Kashi Y Adult non-biting midges: possible windborne carriers of *Vibrio cholerae* non-O1 non-O139. Environ Microbiol 7, 576–585 (2005). [PubMed: 15816934]
19. Halpern M, Raats D, Lavion R & Mittler S Dependent population dynamics between chironomids (nonbiting midges) and Vibrio cholerae. FEMS Microbiol Ecol 55, 98–104 (2006). [PubMed: 16420618]
20. Echeverria P, Harrison BA, Tirapat C & McFarland A Flies as a source of enteric pathogens in a rural village in Thailand. Applied and environmental microbiology 46, 32–36 (1983). [PubMed: 6351748]
21. Fotedar R Vector potential of houseflies (Musca domestica) in the transmission of Vibrio cholerae in India. Acta Trop 78, 31–34 (2001). [PubMed: 11164748]

22. Yildiz FH & Schoolnik GK *Vibrio cholerae* O1 El Tor: identification of a gene cluster required for the rugose colony type, exopolysaccharide production, chlorine resistance, and biofilm formation. Proc Natl Acad Sci U S A 96, 4028–4033 (1999). [PubMed: 10097157]
23. Watnick PI & Kolter R Steps in the development of a *Vibrio cholerae* El Tor biofilm. Mol Microbiol 34, 586–595 (1999). [PubMed: 10564499]
24. Purdy AE & Watnick PI Spatially selective colonization of the arthropod intestine through activation of *Vibrio cholerae* biofilm formation. Proceedings of the National Academy of Sciences of the United States of America 108, 19737–19742 (2011). [PubMed: 22106284]
25. Zhu J et al. Quorum-sensing regulators control virulence gene expression in *Vibrio cholerae*. Proc Natl Acad Sci U S A 99, 3129–3134 (2002). [PubMed: 11854465]
26. Van der Henst C, Scrignari T, Maclachlan C & Blokesch M An intracellular replication niche for Vibrio cholerae in the amoeba Acanthamoeba castellanii. ISME J 10, 897–910 (2016). [PubMed: 26394005]
27. Sun S, Kjelleberg S & McDougald D Relative contributions of Vibrio polysaccharide and quorum sensing to the resistance of Vibrio cholerae to predation by heterotrophic protists. PLoS One 8, e56338 (2013). [PubMed: 23441178]
28. Hoque MM et al. Quorum Regulated Resistance of Vibrio cholerae against Environmental Bacteriophages. Sci Rep 6, 37956 (2016). [PubMed: 27892495]
29. Thelin KH & Taylor RK Toxin-coregulated pilus, but not mannose-sensitive hemagglutinin, is required for colonization by *Vibrio cholerae* O1 El Tor biotype and O139 strains. Infect Immun 64, 2853–2856 (1996). [PubMed: 8698524]
30. Joelsson A, Liu Z & Zhu J Genetic and phenotypic diversity of quorum-sensing systems in clinical and environmental isolates of *Vibrio cholerae*. Infection and immunity 74, 1141–1147 (2006). [PubMed: 16428762]
31. Wang Z, Hang S, Purdy AE & Watnick PI Mutations in the IMD pathway and mustard counter *Vibrio cholerae* suppression of intestinal stem cell division in Drosophila. mBio 4, e00337–00313 (2013). [PubMed: 23781070]
32. Centers for Disease, C. & Prevention Update: outbreak of cholera ---Haiti, 2010. MMWR Morb Mortal Wkly Rep 59, 1586–1590 (2010). [PubMed: 21150867]
33. Chin CS et al. The origin of the Haitian cholera outbreak strain. The New England journal of medicine 364, 33–42 (2011). [PubMed: 21142692]
34. Centers for Disease, C. & Prevention Cholera outbreak --- Haiti, October 2010. MMWR Morb Mortal Wkly Rep 59, 1411 (2010). [PubMed: 21048563]
35. Azarian T et al. Phylodynamic analysis of clinical and environmental Vibrio cholerae isolates from Haiti reveals diversification driven by positive selection. mBio 5 (2014).
36. Vanhove AS et al. *Vibrio cholerae* ensures function of host proteins required for virulence through consumption of luminal methionine sulfoxide. PLoS Pathog 13, e1006428 (2017). [PubMed: 28586382]
37. Plamann MD, Rapp WD & Stauffer GV *Escherichia coli* K12 mutants defective in the glycine cleavage enzyme system. Molecular & general genetics : MGG 192, 15–20 (1983). [PubMed: 6358793]
38. Hang S et al. The acetate switch of an intestinal pathogen disrupts host insulin signaling and lipid metabolism. Cell host & microbe 16, 592–604 (2014). [PubMed: 25525791]
39. Mancusso R, Gregorio GG, Liu Q & Wang DN Structure and mechanism of a bacterial sodium-dependent dicarboxylate transporter. Nature 491, 622–626 (2012). [PubMed: 23086149]
40. Mingrone G & Castagneto M Medium-chain, even-numbered dicarboxylic acids as novel energy substrates: an update. Nutr Rev 64, 449–456 (2006). [PubMed: 17063926]
41. Whereat AF, Hull FE & Orishimo MW The role of succinate in the regulation of fatty acid synthesis by heart mitochondria. J Biol Chem 242, 4013–4022 (1967). [PubMed: 4383531]
42. Chatterjee D et al. Control of metabolic adaptation to fasting by dILP6-induced insulin signaling in Drosophila oenocytes. Proc Natl Acad Sci U S A 111, 17959–17964 (2014). [PubMed: 25472843]
43. Slaidina M, Delanoue R, Gronke S, Partridge L & Leopold P A *Drosophila* insulin-like peptide promotes growth during nonfeeding states. Dev Cell 17, 874–884 (2009). [PubMed: 20059956]

44. Honegger B et al. Imp-L2, a putative homolog of vertebrate IGF-binding protein 7, counteracts insulin signaling in *Drosophila* and is essential for starvation resistance. Journal of biology 7, 10 (2008). [PubMed: 18412985]
45. Okamura T, Shimizu H, Nagao T, Ueda R & Ishii S ATF-2 regulates fat metabolism in *Drosophila*. Mol Biol Cell 18, 1519–1529 (2007). [PubMed: 17314398]
46. Musselman LP et al. A high-sugar diet produces obesity and insulin resistance in wild-type Drosophila. Dis Model Mech 4, 842–849 (2011). [PubMed: 21719444]
47. Selak MA et al. Succinate links TCA cycle dysfunction to oncogenesis by inhibiting HIF-alpha prolyl hydroxylase. Cancer Cell 7, 77–85 (2005). [PubMed: 15652751]
48. Bandarra D, Biddlestone J, Mudie S, Muller HA & Rocha S HIF-1alpha restricts NF-kappaB-dependent gene expression to control innate immunity signals. Dis Model Mech 8, 169–181 (2015). [PubMed: 25510503]
49. Gronke S et al. Brummer lipase is an evolutionary conserved fat storage regulator in *Drosophila*. Cell metabolism 1, 323–330 (2005). [PubMed: 16054079]
50. Peterson JS, Timmons AK, Mondragon AA & McCall K The End of the Beginning: Cell Death in the Germline. Curr Top Dev Biol 114, 93–119 (2015). [PubMed: 26431565]
51. Michie KL, Cornforth DM & Whiteley M Bacterial tweets and podcasts #signaling#eavesdropping#microbialfightclub. Mol Biochem Parasitol 208, 41–48 (2016). [PubMed: 27208877]
52. Jung SA, Chapman CA & Ng WL Quadruple quorum-sensing inputs control Vibrio cholerae virulence and maintain system robustness. PLoS pathogens 11, e1004837 (2015). [PubMed: 25874462]
53. Stutzmann S & Blokesch M Circulation of a Quorum-Sensing-Impaired Variant of Vibrio cholerae Strain C6706 Masks Important Phenotypes. mSphere 1 (2016).
54. Ruby EG & McFall-Ngai MJ A squid that glows in the night: development of an animal-bacterial mutualism. J Bacteriol 174, 4865–4870 (1992). [PubMed: 1629148]
55. Visick KL & Ruby EG *Vibrio fischeri* and its host: it takes two to tango. Curr Opin Microbiol 9, 632–638 (2006). [PubMed: 17049299]
56. McFall-Ngai MJ & Ruby EG Symbiont recognition and subsequent morphogenesis as early events in an animal-bacterial mutualism. Science 254, 1491–1494 (1991). [PubMed: 1962208]
57. Aschtgen MS et al. Rotation of *Vibrio fischeri* Flagella Produces Outer Membrane Vesicles That Induce Host Development. J Bacteriol 198, 2156–2165 (2016). [PubMed: 27246572]
58. Lee KH & Ruby EG Competition between *Vibrio fischeri* strains during initiation and maintenance of a light organ symbiosis. J Bacteriol 176, 1985–1991 (1994). [PubMed: 8144466]
59. Fidopiastis PM, Miyamoto CM, Jobling MG, Meighen EA & Ruby EG LitR, a new transcriptional activator in *Vibrio fischeri*, regulates luminescence and symbiotic light organ colonization. Mol Microbiol 45, 131–143 (2002). [PubMed: 12100554]
60. Tamplin ML, Gauzens AL, Huq A, Sack DA & Colwell RR Attachment of *Vibrio cholerae* serogroup O1 to zooplankton and phytoplankton of Bangladesh waters. Appl Environ Microbiol 56, 1977–1980 (1990). [PubMed: 2383016]
61. El-Bassiony GM, Luizzi V, Nguyen D, Stoffolano JG, Jr. & Purdy AE *Vibrio cholerae* laboratory infection of the adult house fly *Musca domestica*. Med Vet Entomol 30, 392–402 (2016). [PubMed: 27444689]
62. Zhang Z et al. Identification of lysine succinylation as a new post-translational modification. Nat Chem Biol 7, 58–63 (2011). [PubMed: 21151122]
63. Jiang C et al. Disruption of hypoxia-inducible factor 1 in adipocytes improves insulin sensitivity and decreases adiposity in high-fat diet-fed mice. Diabetes 60, 2484–2495 (2011). [PubMed: 21873554]
64. D'Ignazio L, Bandarra D & Rocha S NF-kappaB and HIF crosstalk in immune responses. FEBS J 283, 413–424 (2016). [PubMed: 26513405]
65. Diehl J et al. Expression and localization of GPR91 and GPR99 in murine organs. Cell and tissue research 364, 245–262 (2016). [PubMed: 26590824]

66. He W et al. Citric acid cycle intermediates as ligands for orphan G-protein-coupled receptors. Nature 429, 188–193 (2004). [PubMed: 15141213]

67. Regard JB, Sato IT & Coughlin SR Anatomical profiling of G protein-coupled receptor expression. Cell 135, 561–571 (2008). [PubMed: 18984166]

68. McCreath KJ et al. Targeted disruption of the SUCNR1 metabolic receptor leads to dichotomous effects on obesity. Diabetes 64, 1154–1167 (2015). [PubMed: 25352636]

69. Horton RM et al. Gene splicing by overlap extension. Methods in enzymology 217, 270–279 (1993). [PubMed: 8474334]

70. Metcalf WW et al. Conditionally replicative and conjugative plasmids carrying lacZ alpha for cloning, mutagenesis, and allele replacement in bacteria. Plasmid 35, 1–13 (1996). [PubMed: 8693022]

71. Haugo AJ & Watnick PI *Vibrio cholerae* CytR is a repressor of biofilm development. Mol Microbiol 45, 471–483 (2002). [PubMed: 12123457]

72. Houot L, Chang S, Pickering BS, Absalon C & Watnick PI The phosphoenolpyruvate phosphotransferase system regulates *Vibrio cholerae* biofilm formation through multiple independent pathways. Journal of bacteriology 192, 3055–3067 (2010). [PubMed: 20400550]

73. Smith DR et al. In situ proteolysis of the *Vibrio cholerae* matrix protein RbmA promotes biofilm recruitment. Proceedings of the National Academy of Sciences of the United States of America 112, 10491–10496 (2015). [PubMed: 26240338]

74. Yuan M, Breitkopf SB, Yang X & Asara JM A positive/negative ion-switching, targeted mass spectrometry-based metabolomics platform for bodily fluids, cells, and fresh and fixed tissue. Nat Protoc 7, 872–881 (2012). [PubMed: 22498707]

75. Xia J, Mandal R, Sinelnikov IV, Broadhurst D & Wishart DS MetaboAnalyst 2.0--a comprehensive server for metabolomic data analysis. Nucleic Acids Res 40, W127–133 (2012). [PubMed: 22553367]

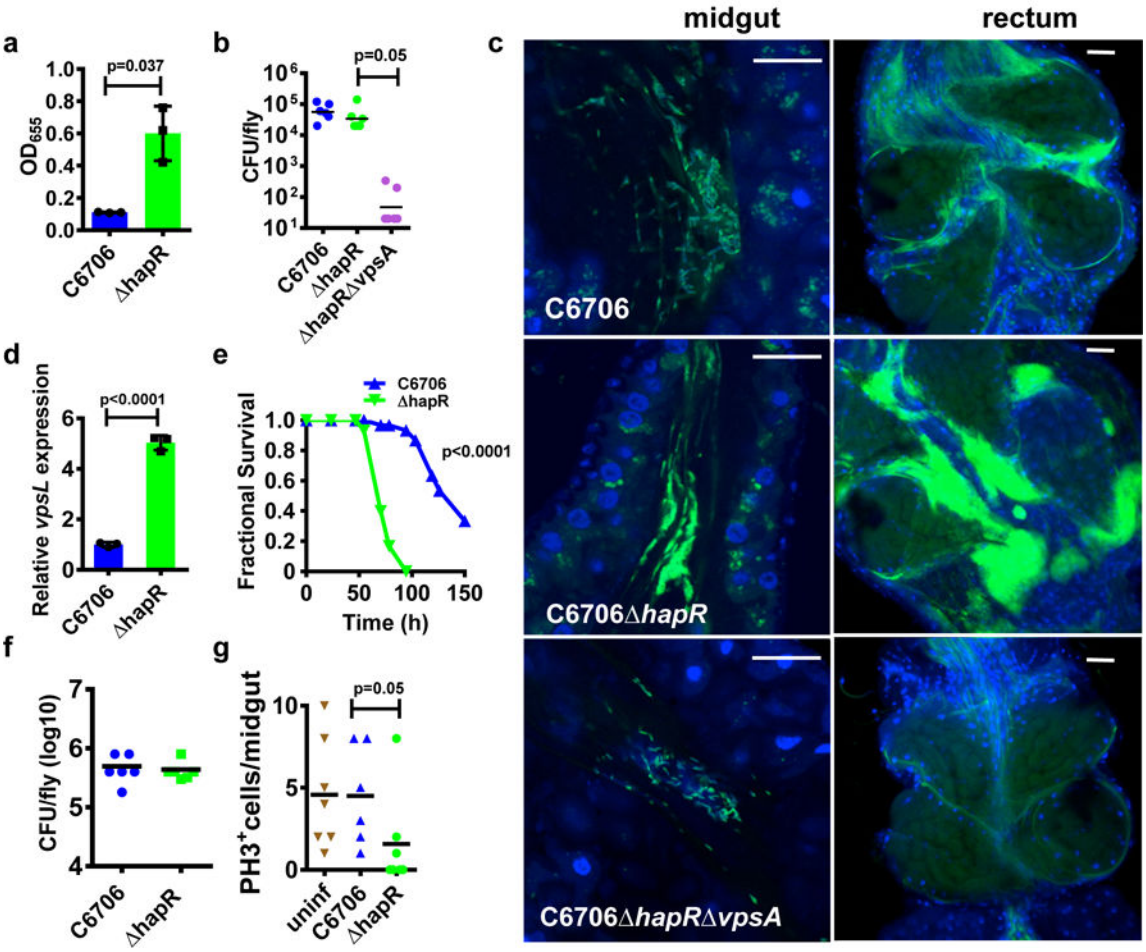

Figure 1: *V. cholerae* high cell density quorum sensing-dependent signaling is activated in the *Drosophila* intestine and promotes host survival of infection.

(a) Comparison of biofilm formation by *V. cholerae* strain C6706 isolated from a Peruvian patient in 1991 and the corresponding Δ*hapR* mutant. Three independent biological replicates were performed. Bars represent the mean measurement, and error bars indicate the standard deviation. A Welch's t-test was used to calculate significance. (b) Average CFU/intestine for *Drosophila* infected for 48 hours with C6706, the corresponding quorum sensing mutant C6706Δ*hapR*, and the double quorum sensing and biofilm mutant C6706Δ*hapR*Δ*vpsA*. Horizontal bars represent the average of six biological replicates. A students t-test was used to calculate significance. (c) Representative micrographs showing the midgut and rectum of flies infected for 48 hours with the indicated *V. cholerae* strains expressing GFP and then washed out for 24 hours. Ten midguts/rectums, each representing an independent biological replicate, were examined. Nuclei were stained with DAPI. Scale bars, 20μm. (d) qRT-PCR measurements of *vpsL* transcription by the indicated *V. cholerae* strains in the *Drosophila* intestine. Three independent biological replicates were performed. Bars indicate the mean measurement, and error bars represent the standard deviation. A student's t test was used to calculate significance. (e) Survival over time of flies infected with the indicated strains. Three cohorts of ten co-housed flies representing three independent biological replicates were used. Statistical significance was calculated by log

rank analysis. (f) Intestinal bacterial burden and (g) $PH3^+$ staining of the indicated *V. cholerae* strains after infection for 48 hours. Horizontal bars represent the average of six to seven biological replicates in (f) and (g). A Mann-Whitney test was used to calculate significance.

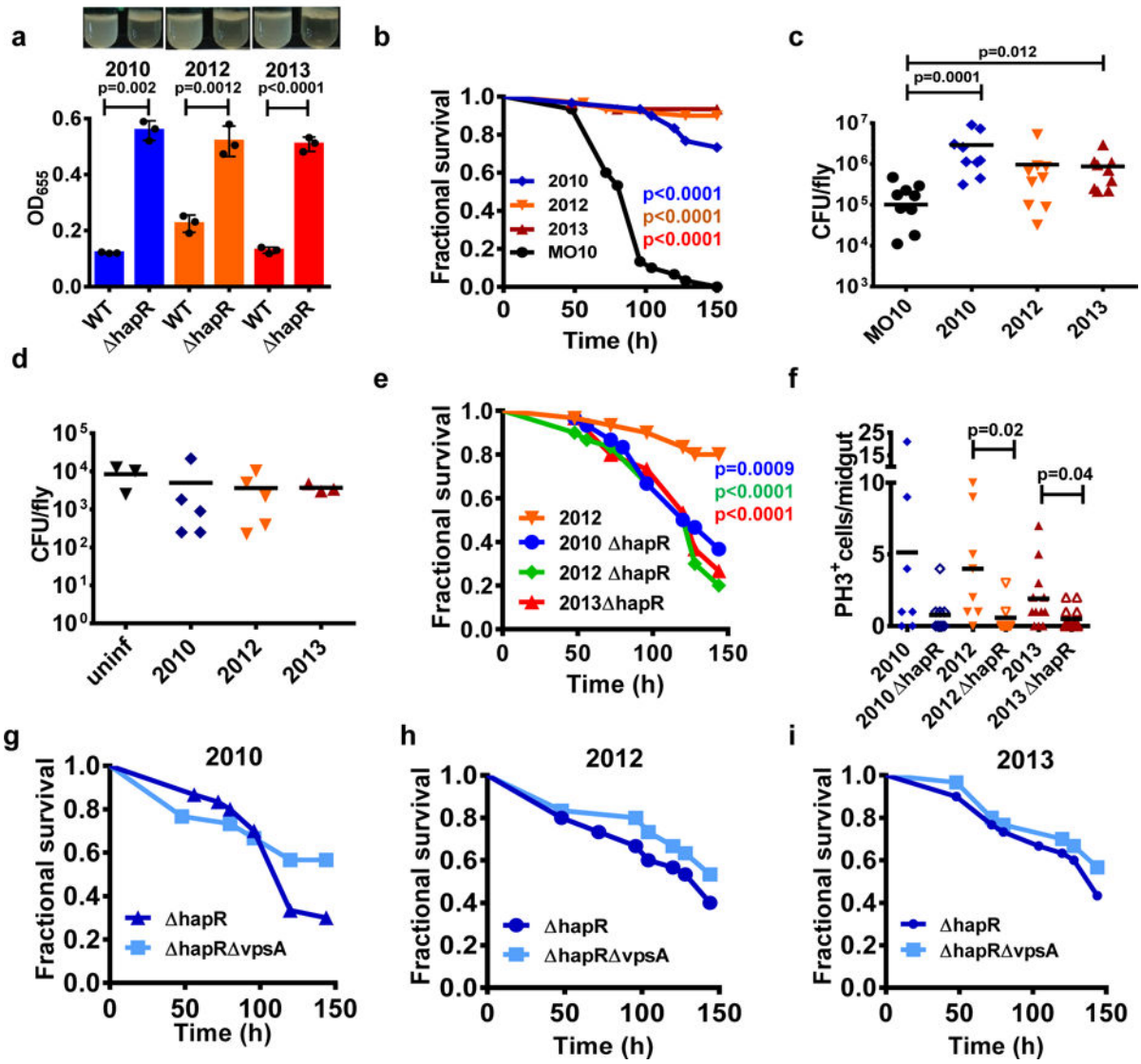

Figure 2: *V. cholerae* quorum sensing promotes host survival independent of biofilm formation.

(a) Comparison of biofilm formation by wild-type *V. cholerae* and the corresponding Δ*hapR* mutants collected from Haiti in the indicated year. Quantification is shown below, and representative biofilm images are shown above. The mean of three independent biological replicates is shown. Error bars represent the standard deviation. A Welch's t-test was used to calculate significance. (b) Survival of flies infected with *V. cholerae* O139 strain MO10 collected during the 1992 epidemic in Southeast Asia and three clinical strains collected in Haiti during 2010, 2012, and 2013. Three cohorts of ten co-housed flies representing independent biological replicates were used. Statistical significance was calculated by log rank analysis. (c) *V. cholerae* burden and (d) commensal burden of uninfected *Drosophila* (uninf) or those infected with the Haitian strains used in (b). Each symbol represents a biological replicate. Horizontal bars represent the mean measurement. A one-way ANOVA using MO10 as a control with Dunnett's multiple comparison test was used to calculate statistical significance. Adjusted p values are reported. (e) Survival of flies infected with the

indicated Δ*hapR* mutant strains. Survival of flies infected with the parental 2012 strain is shown for comparison. Three cohorts of ten co-housed flies representing independent biological replicates were used. Statistical significance was calculated by log rank analysis. (f) Quantification of $PH3^+$ cells in the intestines of flies infected with the indicated strains. Each symbol represents a biological replicate, and horizontal bars represent the mean measurement. A Mann-Whitney test was used to calculate statistical significance. (g-i) Survival of flies infected with either Δ*hapR* or Δ*hapR*Δ*vpsA* mutant *V. cholerae* strains isolated from Haiti in the indicated year. Three cohorts of ten co-housed flies representing three independent biological replicates were used. Statistical significance was calculated by log rank analysis.

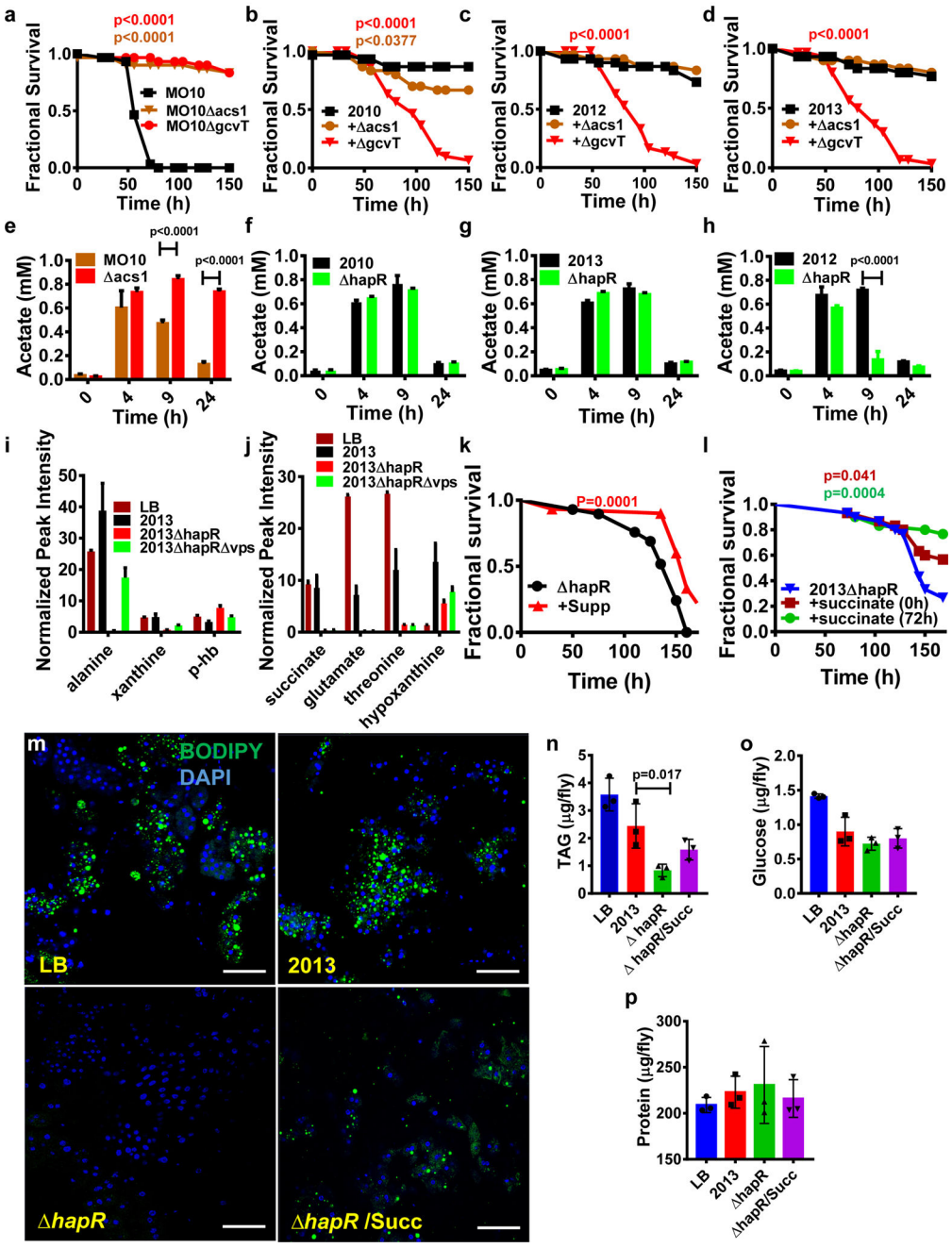

Figure 3: *V. cholerae* quorum sensing and succinate supplementation prevent host lipolysis.

(a) Survival of flies infected with the wild-type *V. cholerae* strain MO10, and the corresponding Δ*gcvT* and Δ*acs1* mutants. (b-d) Survival of flies infected with co-cultures of the indicated Haitian strain and MO10Δ*gcvT* or Δ*acs1* strain. (e-h) Quantification of acetate in the supernatants of the indicated wild-type *V. cholerae* strains and the corresponding Δ*hapR* mutant cultured for the indicated lengths of time. A student's t test was used to calculate significance. (i) Significantly different metabolites present in the spent supernatants of the 2013 Haitian *V. cholerae* strain that are differentially taken up by the Δ*hapR* mutant as compared with the non-biofilm forming wild-type and Δ*hapR*Δ*vpsA*

mutant strains. parahydroxybenzoate (p-hb). (j) Metabolites that are differentially consumed by both the Δ*hapR* and Δ*hapR*Δ*vpsA* mutant strains. A lower peak intensity threshold of 5 was used to eliminate less abundant metabolites. Data was analyzed as described in the text. (k) Survival of flies infected with the Δ*hapR* mutant strain in LB alone or supplemented with 5mM concentrations of succinate, glutamate, and threonine. (l) Survival of flies infected with the Δ*hapR* mutant strain in LB alone (CTL) or supplemented with succinate (5mM) at 0 or 72 hours. (m) Representative micrographs showing Bodipy staining of lipid droplets in the fat bodies of flies exposed for 4 days to LB broth alone or inoculated with *V. cholerae* from 2013, the corresponding *ΔhapR* mutant, or the corresponding *ΔhapR* mutant supplemented with succinate. Ten fat bodies, each representing an independent biological replicate, were examined. Scale bars, 50μm. Quantification of (n) total triglycerides, (o) total glucose, and (p) total protein in flies treated as described in a-d. Three cohorts of ten co-housed flies representing independent biological replicates were used. A one-way ANOVA using 2013 as a reference with Dunnett's multiple comparison test was used to calculate statistical significance. For all bar graphs, bars represent the mean of three independent biological replicates, and error bars represent the standard deviation. For all survival experiments, three cohorts of ten co-housed flies representing independent biological replicates were used. Statistical significance was calculated by log rank analysis.

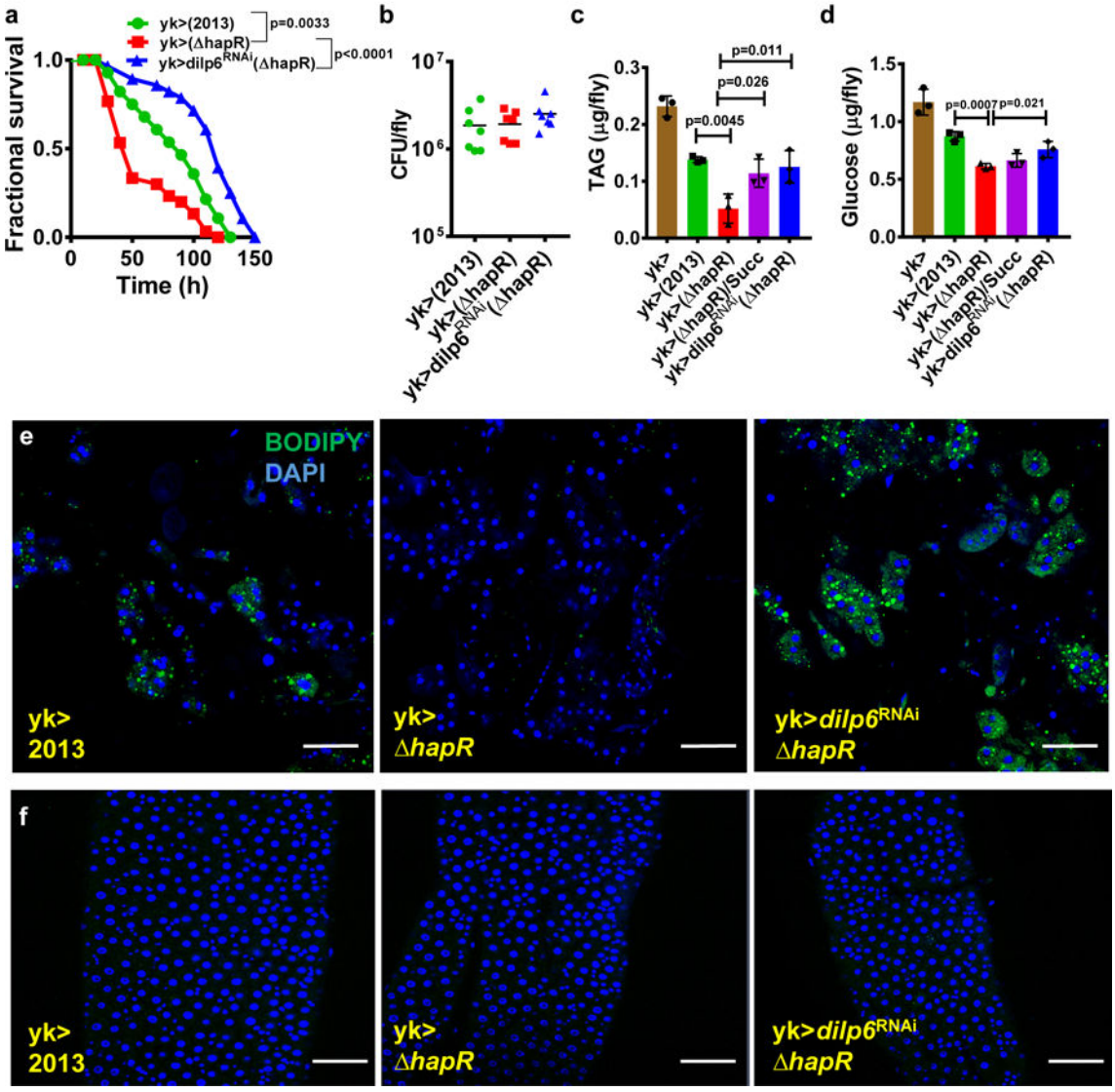

Figure 4: *dilp6* knockdown inhibits host infection-induced lipolysis and prolongs host survival.

(a) Survival of flies with the indicated genotypes infected with the indicated *V. cholerae* strains. Dilp6^{RNAi} construct 111727 was used. Three cohorts of ten co-housed flies representing independent biological replicates were used. P values, corresponding to the relevant comparisons, are indicated on the graph. Log rank analysis was used to assess significance. (b) *V. cholerae* burden per fly for the indicated bacterial and *Drosophila* strains. Horizontal bars represent the mean. Seven cohorts of ten co-housed flies representing independent biological replicates were used. Statistical significance was calculated using a one way ANOVA with Dunnett's multiple comparison test. (c)Total triglycerides and (d) total glucose in the indicated bacterial and *Drosophila* strains. Three biological replicates were performed. Bars represent the mean, and error bars represent the standard deviation. A one-way ANOVA using Δ*hapR* as a reference with Dunnett's multiple comparison test was used to calculate statistical significance. An adjusted p value is given. Representative micrographs showing Bodipy staining of lipid droplets in (e) the fat bodies and (f) midguts

of flies carrying yolk-Gal4 (yk) with or without UAS-*dilp6* ^{RNAi} (VDRC strain 111727) and infected with *V. cholerae* (2013) or *V. cholerae*Δ*hapR* (Δ*hapR*). Nuclei are stained with DAPI. Ten fat bodies/midguts, each representing an independent biological replicate were examined. Scale bars, 50μm.